Naval Research Laboratory
Stennis Space Center, MS 39529-5004

NRL/FR/7322--97-9669

Review and Verification of Numerical Wave Models for Near Coastal Areas – Part 1: Review of Mild Slope Equation, Relevant Approximations, and Technical Details of Numerical Wave Models

JAMES M. KAIHATU

Ocean Dynamics and Prediction Branch
Oceanography Division

November 7, 1997

REPORT DOCUMENTATION PAGE

Form Approved
OBM No. 0704-0188

1. AGENCY USE ONLY *(Leave blank)*	2. REPORT DATE	3. REPORT TYPE AND DATES COVERED
	November 7, 1997	Final

4. TITLE AND SUBTITLE
Review and Verification of Numerical Wave Models For Near Coastal Areas – Part 1: Review of Mild Slope Equation, Relevant Approximations, and Technical Details of Numerical Wave Models

5. FUNDING NUMBERS
Job Order No. 573672000
Program Element No. 0602435N
Project No.
Task No. BE-35-2-15
Accession No. DN163783

6. AUTHOR(S)
James M. Kaihatu

7. PERFORMING ORGANIZATION NAME(S) AND ADDRESS(ES)
Naval Research Laboratory
Oceanography Division
Stennis Space Center, MS 39529-5004

8. PERFORMING ORGANIZATION REPORT NUMBER
NRL/FR/7322--97-9669

9. SPONSORING/MONITORING AGENCY NAME(S) AND ADDRESS(ES)
Office of Naval Research
800 N. Quincy St.
Arlington, VA 22217-5000

10. SPONSORING/MONITORING AGENCY REPORT NUMBER

11. SUPPLEMENTARY NOTES

12a. DISTRIBUTION/AVAILABILITY STATEMENT
Approved for public release; distribution unlimited.

12b. DISTRIBUTION CODE

13. ABSTRACT *(Maximum 200 words)*

Ocean wave propagation is heavily affected by bathymetric variation, particularly in the nearshore areas. In this report, the theoretical basis behind the mild slope equation, which is often used for modeling wave propagation, is discussed. In particular, the theory and technical details of the models REF/DIF1, REF/DIF-S, and RCPWAVE are defined. (REF/DIF-S is an irregular wave version of REF/DIF1.) Two different modifications of the mild slope equation that simplify the modeling of wave propagation for general areas: the parabolic approximation, which is used in the model REF/DIF1 and REF/DIF-S; and the eikonal-transport equations, used in RCPWAVE are examined. The consequences of using either modification is also discussed. Incorporation of relevant physical effects (e.g., wave breaking, bottom friction, etc.) that affect wave propagation in the nearshore area is illustrated.

14. SUBJECT TERMS
wave modeling, tide modeling, coupled waves, coupled tides

15. NUMBER OF PAGES
30

16. PRICE CODE

17. SECURITY CLASSIFICATION OF REPORT	18. SECURITY CLASSIFICATION OF THIS PAGE	19. SECURITY CLASSIFICATION OF ABSTRACT	20. LIMITATION OF ABSTRACT
Unclassified	Unclassified	Unclassified	Same as report

CONTENTS

EXECUTIVE SUMMARY

Ocean wave propagation is heavily affected by bathymetric variation, particularly in the nearshore areas. In this report, the theoretical basis behind the mild slope equation, which is often used for modeling wave propagation, is discussed. In particular, the theory and technical details of the models REF/DIF1, REF/DIF-S, and RCPWAVE are defined. (REF/DIF-S is an irregular wave version of REF/DIF1.) Two different modifications of the mild slope equation that simplify the modeling of wave propagation for general areas: the *parabolic approximation*, which is used in the model REF/DIF1 and REF/DIF-S; and the *eikonal-transport* equations, used in RCPWAVE are examined. The consequences of using either modification is also discussed. Incorporation of relevant physical effects (e.g., wave breaking, bottom friction, etc.) that affect wave propagation in the nearshore area is illustrated. Part 2 of this report will describe the verification of these models with analytical solutions and data.

REVIEW AND VERIFICATION OF NUMERICAL WAVE MODELS FOR NEAR COASTAL AREAS - PART 1: REVIEW OF MILD SLOPE EQUATION, RELEVANT APPROXIMATIONS, AND TECHNICAL DETAILS OF NUMERICAL WAVE MODELS

1.0 INTRODUCTION

Ocean waves in the nearshore coastal areas undergo significant modulation due to variations in the underlying bathymetry, tidal currents, and wind. The dominant effect for most open coasts is bathymetric variation. Such effects as wave refraction, diffraction, and shoaling are caused by these variations. Wave *refraction* is the bending of wave crests that occurs as waves (approaching the beach at an angle) move from deeper water to shallow water; different sections of the wave crests are at different depths, and thus, varying phase velocities exist along the crest. The practical result of refraction is that waves approaching the shore at an angle will have a smaller approach angle as it moves up the slope. Wave *shoaling* is a special case of wave refraction, in which the waves approach the beach in a shore normal direction (zero approach angle) in deep water. Both refraction and shoaling account for wave energy propagation in the direction of wave propagation. Wave *diffraction*, in contrast, is a process by which wave energy propagates in a direction perpendicular to the dominant wave direction. Diffraction is responsible for wave propagation behind a breakwater or other structure; in this case, the area behind the breakwater is a *geometric shadow zone* that can only be disturbed by the incident wave due to diffraction. Diffraction is also dominant in areas where pure refraction theory becomes invalid. For example, when waves propagate over a submerged shoal, refraction causes a focusing of wave energy in the lee of the shoal. Pure refraction theory would predict an infinite wave height in the focus region. In fact, wave diffraction allows energy to "leak" in the direction along the wave crests. A complete description of these effects is beyond the scope of this report. The interested reader is referred to such textbooks as Dean and Dalrymple (1984) for further information.

For particular bathymetric configurations, analytic solutions exist; however, for general wave propagation scenarios, numerical modeling is utilized. There are several governing equations that can simulate this propagation; one of the most popular is the mild slope equation of Berkhoff (1972) and Smith and Sprinks (1975). With it, the combined effect of wave refraction and diffraction can be simulated.

In this report, three combined refraction-diffraction models (two monochromatic models and one spectral model) that the Navy utilizes are discussed. The monochromatic models are REF/DIF1 (version 2.5), a parabolic approximation of the mild slope equation developed by J. T. Kirby and R. A. Dalrymple of the University of Delaware, and RCPWAVE, a forward propagating wave model developed by B. Ebersole of the Coastal Engineering Research Center (now the Coastal and Hydraulics Laboratory), U.S. Army Corps of Engineers Waterways Experiment Station. Also discussed is the model REF/DIF-S (version 1.2), developed by J. T. Kirby, H. T. Ozkan, and A. Chawla of the Center for Applied Coastal Research, University of Delaware. REF/DIF-S is a spectral version of REF/DIF1 in that it can take many frequencies and directions and run them

simultaneously over the domain to simulate the propagation of an irregular wave field. Both REF/DIF1 and REF/DIF-S are fairly recent arrivals to the Navy's arsenal of wave models, while RCPWAVE has served as the wave transformation component of the Navy Standard Surf Model. Information on the operation of these models can be found in the following publications: Kirby and Dalrymple (1994) (REF/DIF1); Ebersole et al. (1986) (RCPWAVE); and Kirby and Ozkan (1994) (REF/DIF-S). Note here that the report by Kirby and Ozkan (1994) describes REF/DIF-S version 1.1; this version differs from version 1.2 in the use of name lists and some details in the calculation of angles. No user's manual has yet been issued for version 1.2, though some details on REF/DIF-S version 1.2 can be found in Chawla (1995).

Because nearshore wave modeling is a fairly recent Navy research focus, some discussion about wave modeling in general is also included, particularly with respect to mild slope equation models. This discussion will provide a foundation from which the individual specific models can be described. This report is not intended to replace the user's documentation referenced above. Its purpose is to examine, in some detail, some of the theoretical aspects behind the wave models. It is hoped that this review will aid the user in determining the model(s) range of applicability.

2.0 THEORY

2.1 Classes of Wave Models

Most numerical models for wave propagation can be divided into two broad classes: *phase averaged* and *phase resolving*. *Phase averaged* models are expressed in terms of the evolution of a conserved quantity such as wave energy or (in the case of currents) wave action. These models are expressible essentially as an energy balance, where various source terms (such as generation of waves due to wind) and sink terms (energy dissipation due to whitecapping, bottom friction, etc.) are added to the models and tracked as the wave spectra propagates onshore. Models in this realm include WAM (WAve Model) (e.g., Komen et al. 1994), SWAN (Simulating WAves Nearshore) (e.g., Holthuijsen et al. 1993) and STWAVE (e.g., Resio 1988). On an operational basis, many of these models are valuable for propagating waves over global distances to shelf regions; several laboratories have global WAM predictions running continuously. However, their formulations do not include the fine-scale propagation effects that strongly influence the wave field in the nearshore and coastal areas. *Phase resolving* models are formulated in terms of the free surface. These models are derived from the governing equations of fluid mechanics, and since they treat the wave as a deterministic (rather than statistical) quantity they can offer physically consistent simulations of fine-scale variations in the nearshore area due to bathymetric and current effects.

2.2 Mild Slope Equation

The models discussed herein for the most part are based on the mild slope equation of Berkhoff (1972) and Smith and Sprinks (1975). That of Smith and Sprinks (1975) reads:

$$\frac{\partial^2 \phi}{\partial t^2} \nabla \bullet \left(CC_g \nabla \phi \right) + \left(\omega^2 - k^2 CC_g \right) \phi = 0 \,, \tag{2.1}$$

where C is the phase velocity, C_g the group velocity, k is the wavenumber, ω is the wave frequency, and ϕ is the velocity potential, which exists for inviscid irrotational flows. The gradient operator

∇ is applicable in the two horizontal dimensions only; the equation is depth-integrated. Figure 1 shows the definition of the domain and the orientation of the coordinate axes for both REF/DIF1 and RCPWAVE. We also add the assumption that our flow is incompressible. The wave frequency and phase velocities are related by the linear dispersion relation for water waves

$$C = \frac{\omega}{k} = \sqrt{\frac{gk \tanh kh}{k^2}} \ . \tag{2.2}$$

Earlier, Berkhoff (1972) derived the mild slope equation for time-periodic waves, an assumption not employed by Smith and Sprinks (1975). The mild slope equation of Berkhoff (1972) reads

$$\nabla \bullet \left(CC_g \nabla \hat{\phi} \right) + k^2 CC_g \phi = 0 \ , \tag{2.3}$$

where ϕ and $\hat{\phi}$ are related by

$$\phi = \hat{\phi} e^{-i\omega t} \ . \tag{2.4}$$

Berkhoff (1972) derived his mild slope equation by manipulating the Lagrangian for water waves, while Smith and Sprinks (1975) derived their equation by utilizing Green's Second Identity on the velocity potential and the depth dependence. The mild slope equation can simulate wave refraction, diffraction, shoaling, and (if given the proper boundary conditions) reflection from

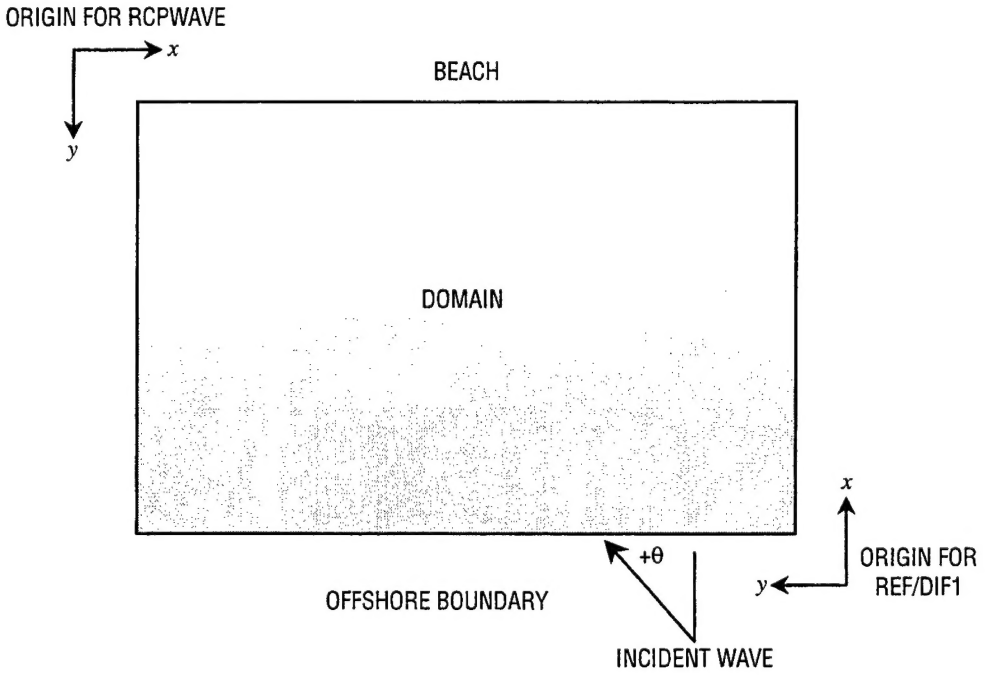

Fig. 1 — Definition of domain and axes orientations for the wave models

structures or steep bathymetry. The asymptotic behavior of the mild slope equation is interesting to examine. Pure diffraction can be recovered by neglecting bottom slopes; this leads to

$$\nabla^2\phi + k^2\phi = 0\,, \tag{2.5}$$

which is the Helmholtz equation. This equation governs waves propagating over a constant depth, where waves are periodic in time but not space, and characteristics are shared by diffracting waves. Specific solutions depend on the imposition of certain boundary conditions. Pure refraction can be recovered by first making the following substitution

$$\phi = \frac{-ig}{\omega} a(x,y) e^{iS(x,y)}\,, \tag{2.6}$$

where a is the wave amplitude and S the wave phase (for a long-crested wave train $S(x,y) = k_x^2 + k_y^2$, where k_x and k_y are the x and y projections of the wavenumber vector). The complex coefficient in (2.6) ensures that a is the amplitude of the free surface elevation and not the velocity potential; this transformation is valid in the linear limit. Substitution into (2.1) and separating real and imaginary parts leads to

$$\frac{1}{CC_g a}\left[\frac{\partial}{\partial x}\left(CC_g\frac{\partial a}{\partial x}\right) + \frac{\partial}{\partial y}\left(CC_g\frac{\partial a}{\partial y}\right)\right] - \left|\nabla S\right|^2 + k^2 = 0 \tag{2.7}$$

and

$$\frac{\partial}{\partial x}\left(CC_g a^2\frac{\partial S}{\partial x}\right) + \frac{\partial}{\partial y}\left(CC_g a^2\frac{\partial S}{\partial y}\right) = 0\,. \tag{2.8}$$

These equations are sometimes referred to as the *eikonal-transport* equations. Neglecting changes in the amplitude a

$$\left(\frac{\partial a}{\partial x}\right) = \left(\frac{\partial a}{\partial y}\right) = 0 \tag{2.9}$$

leads to

$$k^2 - \left(\frac{\partial S}{\partial x}\right)^2 - \left(\frac{\partial S}{\partial y}\right)^2 = 0 \tag{2.10}$$

and

$$\frac{\partial}{\partial x}\left(CC_g a^2 k_x\right) + \frac{\partial}{\partial y}\left(CC_g a^2 k_y\right) = 0\,, \tag{2.11}$$

which are equivalent in form to the ray equations (Munk and Arthur 1952). The mild slope equation assumes that the bathymetry is slowly varying; however, Booij (1983) determined that it is essentially

accurate for slopes up to 1:3. The mild slope equation has been modified to account for wave transformation due to ambient currents; these would be necessary for areas near inlets where ebb and flood currents have a marked effect on the wavefield. The mild slope equation for wave-current interaction is (Kirby 1984)

$$\frac{D^2\phi}{Dt^2} + \left(\nabla \bullet \mathbf{U}\right)\frac{D\phi}{Dt} - \nabla \bullet \left(CC_g \nabla\phi\right) + \left(\sigma^2 - k^2 CC_g\right)\phi = 0 \,, \tag{2.12}$$

where σ is the *intrinsic* wave frequency, **U** is the depth-averaged current velocity vector, and

$$\frac{D}{Dt} = \frac{\partial}{\partial t} + \mathbf{U} \bullet \nabla \tag{2.13}$$

or the convective acceleration derivative. The intrinsic frequency σ is related to the *absolute* frequency ω by

$$\omega = \sigma + \mathbf{k} \bullet \mathbf{U} \,. \tag{2.14}$$

This essentially dictates a Doppler shift in the wave frequency due to the nonstationary domain (i.e., the current). The absolute frequency can be thought of as the frequency a wave interacting with a current has relative to a fixed reference frame, while the intrinsic frequency is what the wave has with respect to a reference frame moving at the speed and direction of the current **U**. In most situations, one specifies the absolute frequency. Wave-related parameters, such as the phase speed and wavenumber, are calculated using the intrinsic frequency.

2.3 Parabolic Approximation

The mild slope equation is an elliptic partial differential equation, and a model based on this equation would require prespecification of all boundaries before solution. This is difficult for most open-coast applications, since the locations of wave breaking are not known in advance. Additionally, the grid resolution required for large-scale regional modeling can be computationally prohibitive (often on the order of small fractions of a wavelength). Nevertheless, there have been several models based on the elliptic mild slope equation directly; all are finite element models. The model HARBD (Chen and Houston 1987) is a finite element wave model based on the mild slope equation and used for evaluating wave climates in harbors. Chen and Houston (1987) state the grid should be no coarser than 6 points per wavelength. The model CGWAVE (Xu et al. 1996) is also a finite element model with a dissipative term that simulates wave decay by iterative solution and specification of the shoreline boundary with a reflection coefficient; the waves are calculated over the domain, then excessive wave heights found by applying the breaking criterion. The domain is solved again with dissipation applied at the locations where waves had broken.

In general, however, the parabolic approximation to the mild slope equation is used to ameliorate the difficulty. The approximation was first applied to the mild slope equation by Radder (1979). In essence, the parabolic approximation makes use of scaling arguments concerning the directionality of the wave propagation to reduce the elliptic mild slope equation to a parabolic equation. This reduces a boundary value problem (where the entire boundary must be specified in advance) to an initial value problem (where only the initial condition and the two lateral conditions need be specified), a great reduction in computational requirements since only two consecutive grid rows

at a time are involved in the computation. (Further details on numerical techniques will be provided in a later section.) Additionally, effects such as wave breaking and surf zone decay can be straightforwardly added. Two of the models in this study, REF/DIF1 and REF/DIF-S, are parabolic models.

The parabolic approximation is made by assuming

$$\hat{\phi} = \frac{-ig}{\omega} \hat{A}(x,y) e^{i\int k(x,y)dx}, \tag{2.15}$$

where $\hat{A}$ is a complex amplitude. This assumes that the wave is propagating primarily in one direction and disallows backward-propagating waves (since the phase accumulates in one direction only). Substituting this into (2.2) yields

$$\frac{\partial}{\partial x}\left[CC_g\frac{\partial \hat{A}}{\partial x}\right] + 2i\left(kCC_g\right)\frac{\partial \hat{A}}{\partial x} + i\frac{\partial\left(kCC_g\right)}{\partial x}\hat{A} + \frac{\partial}{\partial y}\left[CC_g\frac{\partial}{\partial y}\left(\hat{A}e^{i\int k(x,y)dx}\right)\right]e^{-i\int k(x,y)dx} = 0 . \tag{2.16}$$

Instead of using the operator splitting technique of Radder (1979) we will outline the multiple scale approach of Yue and Mei (1980). In this case, the derivatives of $\hat{A}$ are ordered as follows

$$\frac{\partial \hat{A}}{\partial x} = O\left(\varepsilon^2\right) \tag{2.17}$$

$$\frac{\partial \hat{A}}{\partial y} = O(\varepsilon), \tag{2.18}$$

where the ε denotes an ordering parameter and O is the ordering notation. This states that the amplitude $\hat{A}$ can undergo greater variation in the y direction than in the x direction; this follows from the assumption (2.15), which retains the fast wave-like variation in the x direction in the complex exponential. Retaining terms up to $O(\varepsilon^2)$ would allow us to keep the amplitude curvature term with respect to y, thus allowing us to model the slow phase-like variation in y that occurs when the wave is turned at a small angle to the x direction. In addition, since (2.15) states that the waves are propagating primarily in the positive x direction, any changes in the amplitude $\hat{A}$ in the x direction would be primarily due to x derivatives of the bottom h. Thus, the order of x-wise bottom slopes, as well as that of x derivatives of depth-dependent properties (e.g. C, C_g), should also be $O(\varepsilon^2)$. Thus, ordering the first two terms of (2.16) in this manner leads to

$$\varepsilon^4\frac{\partial}{\partial x}\left[\left(CC_g\right)\frac{\partial \hat{A}}{\partial x}\right] << \varepsilon^2\left[2i\left(kCC_g\right)\frac{\partial \hat{A}}{\partial x}\right]. \tag{2.19}$$

If we retain terms up to $O(\varepsilon^2)$, we can neglect the first term of (2.16). What remains is a parabolic equation, with first-order derivatives in x and first- and second-order derivatives in y.

One more transformation needs to be made for the model equation to be complete. We integrated the phase function in the complex exponential in (2.15) in the x direction only; however the wavenumber k in the integrand is a function of x and y. Thus, we must make use of a reference

wavenumber $\bar{k}(x)$, which is at most only a function of x. This reference wavenumber can be defined a number of ways; Kirby and Dalrymple (1983a) take the reference wavenumber as being a single wavenumber at the offshore boundary of the domain, while Lozano and Liu (1980) define it as a wavenumber averaged in the y direction, and so a function of x alone. REF/DIF1 uses the Lozano and Liu (1980) definition. Thus, the amplitude $\hat{A}$ is redefined as

$$\hat{A}(x,y) = A(x,y)\, e^{i\left(\int \bar{k}(x)dx - \int k(x,y)dx\right)} . \tag{2.20}$$

Substituting this into (2.16) and enforcing the assumption (2.19) yields

$$2i\left(kCC_g\right)\frac{\partial A}{\partial x} - 2\left(kCC_g\right)\left(\bar{k}-k\right)A + i\frac{\partial\left(kCC_g\right)}{\partial x}A + \frac{\partial}{\partial y}\left(CC_g\frac{\partial A}{\partial y}\right) = 0 . \tag{2.21}$$

Kirby (1984) has also derived a parabolic equation for wave current interaction

$$\left(C_g+U\right)\frac{\partial A}{\partial x} + V\frac{\partial A}{\partial y} + \frac{\sigma}{2}\left(\frac{\partial}{\partial x}\left(\frac{C_g+U}{\sigma}\right) + \frac{\partial}{\partial y}\left(\frac{V}{\sigma}\right)\right)A - \frac{i}{2\sigma}\frac{\partial}{\partial y}\left(CC_g\frac{\partial A}{\partial y}\right) = 0 . \tag{2.22}$$

This model is valid for weak currents (products of currents were neglected). The model was presented as a correction to the model of Booij (1981), which was derived with an incorrect dynamic free surface boundary condition. Kirby and Dalrymple (1983a), prior to that, derived a parabolic model that did not assume weak currents. The model also includes a nonlinear correction consistent with the self-interaction mode from Stokes theory. This model is

$$\left(C_g+U\right)\frac{\partial A}{\partial x} + V\frac{\partial A}{\partial x} + \frac{\sigma}{2}\left(\frac{\partial}{\partial x}\left(\frac{C_g+U}{\sigma}\right) + \frac{\partial}{\partial y}\left(\frac{V}{\sigma}\right)\right)A - \frac{i}{2\sigma}\frac{\partial}{\partial y}\left(\left(CC_g - V^2\right)\frac{\partial A}{\partial y}\right) \tag{2.23}$$

$$+ i\left(\bar{k}-k\right)\left(C_g-U\right)A - \frac{\sigma k^2}{2}D\left|A\right|^2 A = 0 ,$$

where $\bar{k}$ is the y-averaged wavenumber as before and the coefficient of the nonlinear term D is

$$D = \frac{\cosh 4kh + 8 - 2\tanh^2 kh}{8\sinh^4 kh} . \tag{2.24}$$

2.4 Consequences of the Parabolic Approximation; Wide-Angle Propagation

As stated previously, the parabolic approximation makes use of the assumption that the wave propagates primarily in one direction. This has implications for the use of the model in general situations, particularly in instances where the wave would approach the coast at an oblique angle of incidence to the x coordinate (onshore-offshore direction) of the model grid. In such situations, it can be expected that some error would occur.

Liu (1986) has investigated errors incurred with the use of the parabolic approximation. The analysis is briefly outlined here. First, the following relationship between the complex amplitude A and the free surface η is defined

$$\eta = A(x,y)e^{i\int k dx}. \tag{2.25}$$

Substituting this into (2.21) and assuming a flat bottom yields

$$2i\frac{\partial \eta}{\partial x} + \frac{\partial^2 \eta}{\partial y^2} + 2k^2\eta = 0. \tag{2.26}$$

Possible solutions to (2.26) are sought in the form

$$\eta = ae^{i(k_x x + k_y y)}, \tag{2.27}$$

where the assumption is that the plane wave is propagating in the wavenumber vector $\mathbf{k} = (k_x, k_y)$ direction and that $k_x = k\sin\theta$ and $k_y = k\cos\theta$. Substituting this into (2.26) yields

$$k_y^2 + 2kk_x - 2k^2 = 0. \tag{2.28}$$

Then, the same substitution into the Helmholtz equation (2.5) is performed; this yields

$$k_x^2 + k_y^2 = k^2. \tag{2.29}$$

This curve describes a circle in (k_x,k_y) space and shows the directional characteristics of the mild slope equation. The parabolic approximation is essentially an approximation of this curve. The directional range that one would use with the parabolic approximation is dependent on how much error one is willing to tolerate in using (2.28) as an approximation of (2.29). Kirby (1986a) had analyzed the error incurred in using the parabolic approximation by using (2.27) to calculate (k_y/k) as a function of specified (k_x/k), and comparing it to that calculated from (2.28), the exact solution. He determined that a tolerance of 5% error corresponds to a maximum range of ±42.6° from the x coordinate of the grid and a tolerance of 10% corresponds to an angle of ±49.3°. Note here that it is always possible to rotate the grid for a particular scenario to alleviate this difficulty; the rotation would be done to decrease the angle between the incident wave and the x coordinate of the grid. However, this may not be convenient when one is simulating a spectrum of frequencies and directions.

Booij (1981) and Kirby (1986a; 1986b) have developed corrections to the small-angle parabolic approximation that allow a greater bandwidth (with any set tolerance) of directions about the x axis without relinquishing the initial value nature of the parabolic approximation. The development of Kirby (1986a) is described briefly; full details can be found in the referenced literature. Beginning from (2.29), which is the exact relationship between k_x and k_y as represented in the mild slope equation, $(k_x:/k_y)$ can be solved

$$\frac{k_x}{k} = \left(1 - \left(\frac{k_y}{k}\right)^2\right)^{\frac{1}{2}}. \tag{2.30}$$

This equation, like (2.29), is quadratic in both k_x and k_y; this resulted when the plane wave assumption (2.27) was substituted into (2.5). In the case of parabolic equations, the associated relationship between k_x and k_y must be quadratic in k_y only. One method of developing this relationship is by using Pade approximants to expand the square root term; this leads to

$$\frac{k_x}{k} = \frac{\left(1 - \frac{3}{4}\left(\frac{k_y}{k}\right)^2\right)}{\left(1 - \frac{1}{4}\left(\frac{k_y}{k}\right)^2\right)} . \tag{2.31}$$

The associated differential equation that would result in (2.31) were (2.27) substituted into it can be found by the method of operator correspondence; this leads to

$$2ik\frac{\partial A}{\partial x} + \frac{\partial A}{\partial x} + \frac{i}{2k}\frac{\partial^3 A}{\partial x \partial^2 y} = 0 . \tag{2.32}$$

Note the presence of the mixed derivative in (2.32). This is compared to the lowest-order parabolic equation that would result from a reduction of (2.21) for constant depth

$$2ik\frac{\partial A}{\partial x} + \frac{\partial^2 A}{\partial y^2} = 0 . \tag{2.33}$$

It can be shown that (2.32) can be treated by the same numerical techniques as those for (2.33); thus, the mixed derivative adds no new numerical difficulties. This was first derived (though in a slightly different manner) by Booij (1981), who went on to derive a parabolic model that could simulate wave-current interaction. Kirby (1984) corrected an error in Booij's derivation, and derived a model for wave-current interaction from the corrected equation. Kirby (1986a) determined that the Pade approximation yielded improvements on the small-angle parabolic model; a tolerance of 5% error on the calculation of k_x using (2.31) corresponds to an angle bandwidth of ±55.9° and a 10% error can be obtained from an angle of ±61.5°. Figure 2 shows the relationships between k_x

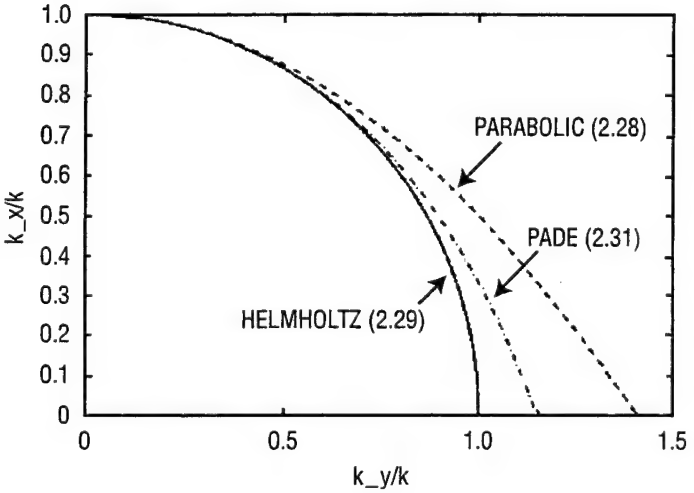

Fig. 2 — Comparison of accuracy of wide-angle propagation characteristics between Helmholtz (exact), small-angle parabolic, and wide-angle (Pade) schemes

and k_y derived from the Helmholtz equation (Eq. 2.29), the small-angle parabolic model (Eq. 2.28), and the wide-angle corrected parabolic model (Eq. 2.31). It is clear that the Pade model better approximates the Helmholtz model for a wider range of k_y (and, thus, a wider range of angles) than the small-angle parabolic model. Kirby (1986a) found that the minimax approximation, rather than the Pade approximation, could yield an even more accurate approximation; however, certain issues concerning high wavenumber noise have as of yet prevented the minimax approximation from being incorporated. The model REF/DIF1 was derived based on the incorporation of wide-angle propagation into Eq. (2.22); the result is

$$\left(C_g+U\right)\frac{\partial A}{\partial x}-2\Delta_1 V\frac{\partial A}{\partial y}+i\left(\bar{k}-a_o k\right)\left(C_g+U\right)A+\left\{\frac{\sigma}{2}\frac{\partial}{\partial x}\left(\frac{C_g+U}{\sigma}\right)-\Delta_1\sigma\frac{\partial}{\partial y}\left(\frac{V}{\sigma}\right)\right\}A \tag{2.34}$$

$$+i\Delta\frac{\partial}{\partial y}\left[\left(CC_g-V^2\right)\frac{\partial}{\partial y}\left(\frac{A}{\sigma}\right)\right]-i\Delta_1\left\{\frac{\partial}{\partial x}\left[UV\frac{\partial}{\partial y}\left(\frac{A}{\sigma}\right)\right]+\frac{\partial}{\partial y}\left[UV\frac{\partial}{\partial x}\left(\frac{A}{\sigma}\right)\right]\right\}$$

$$+\frac{i\sigma k^2}{2}D|A|^2A+\frac{w}{2}A-\frac{b_1}{k}\left\{\frac{\partial^2}{\partial x\partial y}\left[\left(CC_g-V^2\right)\frac{\partial}{\partial y}\left(\frac{A}{\sigma}\right)\right]+2i\frac{\partial}{\partial x}\left(\sigma V\frac{\partial}{\partial y}\left(\frac{A}{\sigma}\right)\right)\right\}$$

$$+b_1\beta\left\{2i\omega U\frac{\partial}{\partial x}\left(\frac{A}{\sigma}\right)+2i\sigma V\frac{\partial}{\partial y}\left(\frac{A}{\sigma}\right)\right\}-b_1\beta\left\{2UV\frac{\partial^2}{\partial x\partial y}\left(\frac{A}{\sigma}\right)+\frac{\partial}{\partial y}\left[\left(CC_g-V^2\right)\frac{\partial}{\partial y}\left(\frac{A}{\sigma}\right)\right]\right\}$$

$$-\frac{ib_1}{k}\left\{\frac{\partial}{\partial y}(\omega V)+3\frac{\partial}{\partial x}(\omega U)\right\}\frac{\partial}{\partial x}\left(\frac{A}{\sigma}\right)-\Delta_2\left\{\omega U\frac{\partial}{\partial x}\left(\frac{A}{\sigma}\right)+\frac{1}{2}\omega\frac{\partial U}{\partial x}\left(\frac{A}{\sigma}\right)\right\}$$

$$+ik\omega U\left(a_o-1\right)\left(\frac{A}{\sigma}\right)=0,$$

where

$$\beta=\frac{1}{k^2}\frac{\partial k}{\partial x}+\frac{1}{2k^2(CC_g-U^2)}\frac{\partial(CC_g-U^2)}{\partial x} \tag{2.35}$$

$$\Delta_1=a_1-b_1 \tag{2.36}$$

$$\Delta_2=1+2a_1-2b_1 \tag{2.37}$$

$$\Delta'=a_1-b_1\frac{\bar{k}}{k}, \tag{2.38}$$

and a_0, a_1, and b_1 are coefficients that control the wide-angle approximation. Setting $\{a_0, a_1, b_1\} = \{1,-0.5,0\}$ yields the small-angle parabolic model of Radder (1979), while setting $\{a_0, a_1, b_1\} = \{1, -0.75,-0.25\}$ yields the Pade wide-angle model of Booij (1981).

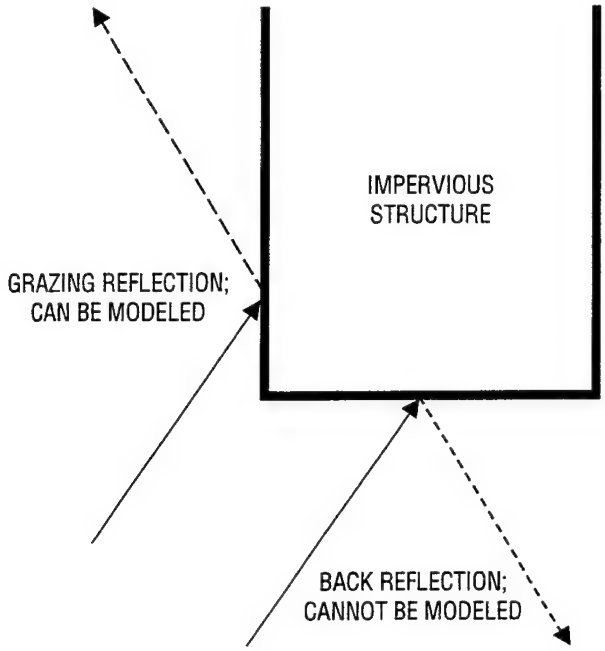

Fig. 3 — Back reflection vs. grazing reflection. Solid arrows show incident wave direction, dashed arrows show reflected wave direction.

A further consequence of the parabolic approximation is the neglect of backward-propagating reflection. For most open-coast situations, this is not a concern; it is not anticipated that the reflection from a beach is significant. The importance of reflection is less clear when islands are present in the domain. The neglect of backward-propagating reflection is more grave in the area of coastal structures. In these instances, only grazing reflection (oblique incidence) can be modeled with parabolic models, and even then, only if the structure is oriented in the cross-shore direction so that the reflected wave is still propagating forward. Figure 3 shows these scenarios.

2.5 An Alternative Formulation: RCPWAVE

A few aspects of the parabolic approximation have been described upon which the model REF/DIF1 is based. It can be argued that considering the small-angle restriction on the parabolic approximation, a less restrictive model can be derived from the Eqs. (2.7) and (2.8), which are not parabolic. If consideration is limited to forward-propagating waves, (2.7) and (2.8) can be solved fairly easily. This is the basis of RCPWAVE (Ebersole 1985; Ebersole et al. 1986). The treatment of Ebersole (1985) will be outlined here. Consideration of only forward-propagating waves implies that RCPWAVE also cannot model back reflection.

Equations (2.7) and (2.8) make up part of the governing equations for RCPWAVE; however, some restriction on the gradient of the phase function S must be set. This condition is the irrotationality of the phase function gradient,

$$\nabla \times (\nabla S) = 0 \tag{2.39}$$

which follows from the mathematical identity that states that the curl of a gradient is zero. If we allowed

$$\nabla S = |\nabla S| \cos\theta \vec{\mathbf{i}} + |\nabla S| \sin\theta \vec{\mathbf{j}} \ , \tag{2.40}$$

where $\vec{\mathbf{i}}$ and $\vec{\mathbf{j}}$ are unit vectors, (2.39) can be rewritten as

$$\frac{\partial}{\partial x}\left(|\nabla S| \sin\theta\right) - \frac{\partial}{\partial y}\left(|\nabla S| \cos\theta\right) = 0 \ . \tag{2.41}$$

Substituting (2.41) into (2.8) yields

$$\frac{\partial}{\partial x}\left(a^2 C C_g |\nabla S| \cos\theta\right) + \frac{\partial}{\partial y}\left(a^2 C C_g |\nabla S| \sin\theta\right) = 0 \ . \tag{2.42}$$

Equations (2.7), (2.41), and (2.42) comprise the model, solving for the wave amplitude a, the wave angle θ, and the magnitude of the phase function gradient $|\nabla S|$ (in fact, the model RCPWAVE solves for the wave height H ($=2a$)). Numerical considerations in solving these sets of equations will be discussed in a later section. In comparing his model to data, Ebersole (1985) explained certain discrepancies between the data and the model as being due to numerical dissipation; however, Kirby (1988) showed that the discrepancies evidenced in the comparisons are more due to the form of the governing Eq. (2.7) rather than any numerical consideration.

3.0 NUMERICAL CONSIDERATIONS

3.1 Parabolic Models

As was previously stated, parabolic models have certain numerical advantages in approximating the full elliptic equations. In this section, these will be outlined in some detail.

Parabolic equations can be solved as initial value problems, requiring only initial and lateral boundary conditions. As mentioned before, this is useful because no down-wave boundary conditions need be specified. As will be described in a later section, this is helpful if wave breaking and decay were to be incorporated into the model.

Numerically, there are several techniques that can be used for solution. These include FTCS (Forward Time Centered Space), Dufort-Frankel, and Crank-Nicholson schemes. The model REF/DIF1 uses the Crank-Nicholson scheme. This is an unconditionally stable implicit scheme with second-order accuracy in both x and y. This finite difference scheme can be shown by applying it to the following parabolic equation

$$\frac{\partial A}{\partial x} = \beta \frac{\partial^2 A}{\partial y^2}, \tag{3.1}$$

where β is a diffusion coefficient. The Crank-Nicholson method consists of a forward difference on the first-order derivative and a centered difference on the second-order derivative. This is done at both row i and row $i + 1$, thus centering the scheme around $i + 1/2, j$. This leads to

$$\frac{A_j^{i+1} - A_j^i}{\Delta x} = \frac{\beta}{2}\left[\left(\frac{A_{j+1}^{i+1} - 2A_j^{i+1} + A_{j-1}^{i+1}}{\Delta y^2}\right) + \left(\frac{A_{j+1}^{i} - 2A_j^{i} + A_{j-1}^{i}}{\Delta y^2}\right)\right]. \tag{3.2}$$

This can be rewritten as

$$-rA_{j+1}^{i+1} + (2+2r)A_j^{i+1} - rA_{j-1}^{i+1} = rA_{j+1}^{i} + (2-2r)A_j^{i} + rA_{j-1}^{i}, \tag{3.3}$$

where

$$r = \frac{\beta \Delta x}{\Delta y^2}. \tag{3.4}$$

In this manner, the unknowns at $i + 1$ can be solved in terms of known values at i. Figure 4 shows the computational molecule that outlines the scheme. It is apparent that the scheme requires only two grid rows in the x direction at a time. This is a savings in memory requirements, since once information is calculated along row $i + 1$, information along row i can be discarded. The matrix size, then, depends only on the number of y (longshore) points. (Note here that this is only true for REF/DIF1; the irregular wave model REF/DIF-S stacks the matrix in this manner for each frequency and direction component modeled, tagging the banded matrix for a particular frequency and direction component onto the end of the matrix for the previous component.) It is also apparent that the molecule requires 6 points, only 3 of which are known. This is the nature of implicit schemes; rather than solving directly for an unknown, one builds a matrix of equations that must be solved. Figure 5 shows the matrix that the method builds. Fortunately, the matrix is tridiagonal in nature, which allows the use of efficient solution techniques such as the Thomas algorithm (Carnahan et al. 1969).

3.2 Numerical Procedures for RCPWAVE

The numerical solution techniques for RCPWAVE are somewhat different, since it is not a parabolic equation. The Crank-Nicholson scheme detailed above is very popular for parabolic equations; however, for Eqs. (2.7), (2.40), and (2.41), the numerical scheme is somewhat more complicated. Full details of the scheme can be found in Ebersole et al. (1986); it will be outlined briefly here. Equations (2.40) and (2.41) can be written generically as

$$\frac{\partial F}{\partial x} + \frac{\partial G}{\partial y} = 0 . \tag{3.5}$$

In contrast to REF/DIF1, which takes the spatially varying wave parameters (wavenumber, water depth, etc.) at the gridpoints (as seen in Fig. 1), RCPWAVE uses a staggered grid, where the center of each grid cell is where wave parameters are taken. This is shown in Fig. 6. In this manner, the x discretization of Eq. (3.5) can be second order with a simple forward step, since this forward

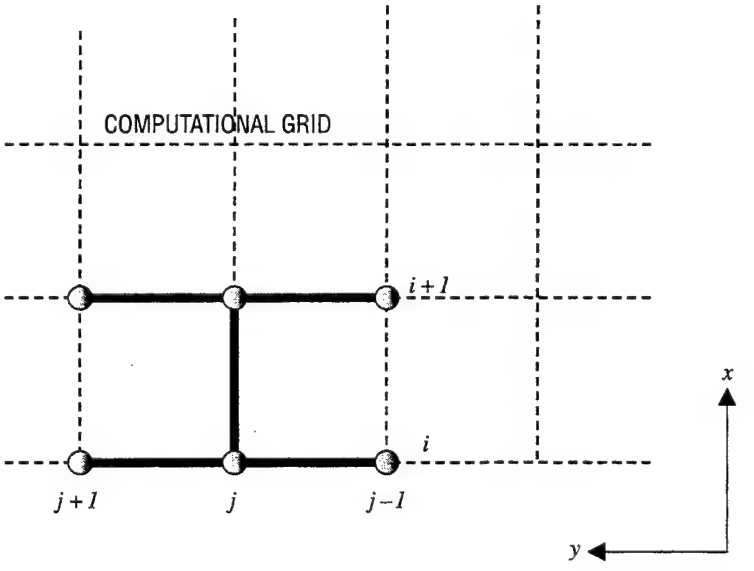

Fig. 4 — Grid definition for REF/DIF1 and Crank-Nicholson computational molecule for i,j gridpoint.

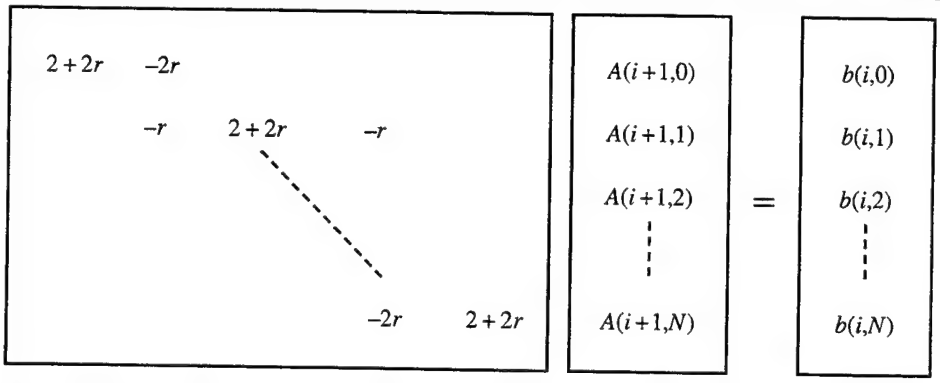

Fig. 5 — Graphical representation of matrix built by Crank-Nicholson method and solved by Thomas algorithm at every step in x. The variable b represents function of known amplitudes at step i. The variable N represents the number of y gridpoints at each row in x.

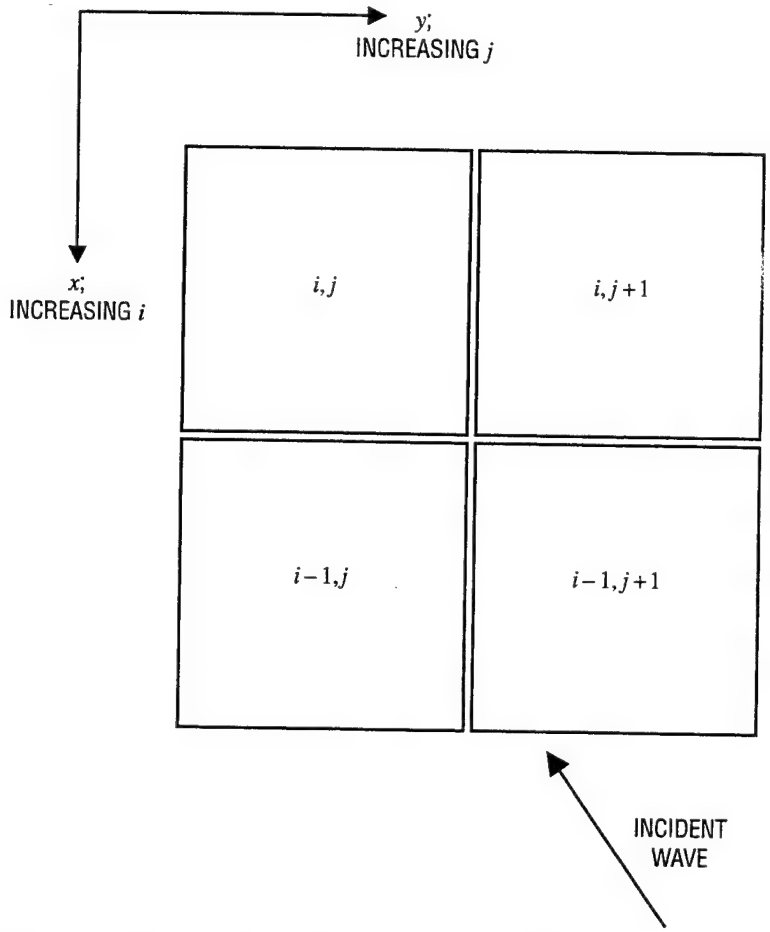

Fig. 6 — Grid cell definition for RCPWAVE. Indices inside cell are defined at cell centers.

step is actually a centered difference about the point $i + 1/2, j$. This is also true of REF/DIF1; however, rather than explicitly staggering the grid, REF/DIF1 averages the spatially varying wave parameters between i and $i + 1$, thus locating them at $i + 1/2, j$ and making the forward step actually a centered difference.

The scheme used to solve Eq. (3.5) is

$$F_j^{i-1} = \Lambda F_{j-1}^{i} + (1-2\Lambda) F_j^{i} + \Lambda F_{j-1}^{i} + \Delta x \left[W \left(\frac{G_{j+1}^{i-1} - G_{j-1}^{i-1}}{2\Delta y} \right) + (1-W) \left(\frac{G_{j+1}^{i} - G_{j-1}^{i}}{2\Delta y} \right) \right], \quad (3.6)$$

where Λ is a "dissipative interface" included to enhance numerical stability and W is a weighting factor that determines the partitioning between explicit and implicit solutions. In RCPWAVE, $\Lambda = 0.167$ and $W = 1.0$ (thus, fully implicit). Equation (3.6) is solved for the unknown value at $i-1$. (Recall from Fig. 1 that the origin of RCPWAVE is on land; the waves propagate from maximum i to $i = 1$.) The finite difference form of Eq. (2.40) can be derived by making the following substitutions

$$F = |\nabla S| \sin \theta \quad (3.7)$$

$$G = -|\nabla S| \cos \theta , \quad (3.8)$$

while the following substitutions lead to the finite difference form of Eq. (2.41)

$$F = a^2 C C_g |\nabla S| \cos \theta \quad (3.9)$$

$$G = a^2 C C_g |\nabla S| \sin \theta . \quad (3.10)$$

Equation (2.7) is also discretized by using second-order backward differences on the x derivatives and centered differences on the y derivatives. This can be problematic when the model is less than four gridpoints away from the offshore boundary.

Once the equations are discretized, they are solved in an iterative manner. Recall that Eq. (2.7) is essentially an expression for wavenumber modified by diffraction; thus, a logical first guess for iteration would be a purely refractive wave condition. This would be true for all the wave parameters to be calculated. Snell's Law for wave propagation over a planar slope is used for the first guess

$$\frac{\sin \theta}{C} = \frac{\sin \theta_o}{C_o} , \quad (3.11)$$

where the subscript o refers to a deep-water condition. This gives a first guess for the wave angle. Wave heights are estimated by using refraction and shoaling over a plane slope

$$H = H_o K_r K_s , \quad (3.12)$$

where K_r, the refraction coefficient, is given by

$$K_r = \left(\frac{\cos \theta_o}{\cos \theta} \right) \tag{3.13}$$

and K_s, the shoaling coefficient, is

$$K_s = \left(\frac{1}{\left(1 + \frac{2kh}{\sinh 2kh} \right) \tanh kh} \right)^{\frac{1}{2}}. \tag{3.14}$$

This, along with the dispersion relation, gives initial estimates for the wavenumbers, wave angles, and wave heights all over the domain. Equation (2.41) is then used to calculate the sine of the wave angle, and then Eq. (2.42) is used to calculate wave heights. Iteration between these equations is then commenced until the angles and heights agree between iterations to some predetermined tolerance. Equation (2.7) is then used to calculate the "true" wavenumber, since the preceding calculations have used the wavenumber unaffected by diffraction. With this estimate of wavenumber modified by diffraction, Eqs. (2.41) and (2.42) are then iteratively solved again, until the wavenumber calculation between iterations meets some tolerance. The model then proceeds to the next step forward, using the wave parameters due purely to refraction as an initial guess.

4.0 MODEL FEATURES

In this section, some of the features of these two models will be discussed. These features are apart from those inherent in the mild slope equations and their corresponding variants featured above.

4.1 Features in REF/DIF1

4.1.1 Energy Dissipation

The model REF/DIF1 has the ability to dissipate wave energy due to several physical mechanisms. These include dissipation due to wave breaking, surface films, bottom friction, and the presence of either a laminar or turbulent boundary layer. These expressions are used in the variable w in Eq. (2.34). This generic form, which allows for simple implementation of various dissipation formulation, was first developed by Dalrymple et al. (1984).

Dissipation and wave height decay due to wave breaking is performed with the model of Dally et al. (1985). This dissipation mechanism simulates energy decay in a propagating bore, and assumes that once breaking has occurred, the energy flux tends toward a stable value; thus, the rate of loss of energy flux depends on the amount of flux over this stable value. Kirby and Dalrymple (1986a) show that for parabolic models the dissipation mechanism should be

$$w = \frac{KC_g \left(1 - \left(\frac{\gamma h}{H} \right)^2 \right)}{h}, \tag{4.1}$$

where K and γ are empirical constants equal to 0.017 and 0.4, respectively, and H is the wave height (equal to $2|A|$). This dissipation mechanism is triggered when the breaking wave height criterion ($H > 0.78h$) is met.

The energy dissipation from wave breaking is by far the dominant mechanism; however, energy dissipation from friction with the bottom boundary and any surface layer may also affect wave evolution. The model has dissipation mechanisms for surface damping due to viscous films, laminar boundary layer damping from the viscous bottom, and turbulent bottom boundary layer damping and damping from porous sand. The expression for the laminar surface layer is (Phillips 1980)

$$w = \frac{\sigma k \sqrt{\nu / 2\sigma}(1 - i)}{\tanh\ kh} \tag{4.2}$$

and for the laminar bottom boundary layer is

$$w = \frac{2\sigma k \sqrt{\nu / 2\sigma}(1 - i)}{\sinh\ kh}, \tag{4.3}$$

where ν is the kinematic viscosity. These dissipation mechanisms do not emerge from the water wave problem naturally, since the fluid is assumed inviscid. The use of boundary layer theory assumes that the damping takes place in a small region near the surface and the bottom, where the no-slip boundary condition can be imposed. It is assumed in this model that the viscous effects incurred by either the surface or the bottom are small enough that distortions to the wavenumber k or wave frequency ω are negligible.

Laminar conditions may be adequate in instances where the near bottom velocities are relatively small (i.e., for deep water and/or small amplitude waves). However, in the near coastal region, the boundary layer damping is expected to be turbulent. This is because high waves and shallow water impart higher near bottom velocities than in deep water, and also the roughness of the sediment in the nearshore becomes more apparent to the flow. Thus, the bottom friction is a function of the square of bottom velocity rather than a linear function of velocity as it is for laminar flow. Expressing the shear stress due to turbulent flow as

$$\tau_{xz} = \frac{\rho f}{8} u_b \left| u_b \right|, \tag{4.4}$$

where τ_{xz} is the bottom shear stress, u_b the bottom velocity, and f the friction factor. The dissipation due to a turbulent bottom boundary layer can be calculated as (Dean and Dalrymple 1984)

$$w = \frac{2\sigma k f \left| A \right| (1 - i)}{3\pi \sinh 2kh \sinh kh}. \tag{4.5}$$

For the model implementation the value $f = 0.01$ is assumed.

Wave propagation over porous sand induces a flow into the seabed. This induced Darcy flow serves as a damping mechanism since continuity must be satisfied at the sea bottom. It can be determined that the dispersion relation associated with waves over a porous seabed is complex; the real part determines the wavenumber for a progressive wave and the imaginary part determines

the damping rate. The real wavenumber can be calculated by Eq. (2.2), while the imaginary wavenumber is found by (Reid and Kajuira 1957)

$$k_i = \frac{2\left(\sigma C_p / \nu\right) k}{2kh + \sinh 2kh}, \tag{4.6}$$

where C_p is the coefficient of porosity (assumed to be $4.5 \times 10^{11}\ m^2$). From this, the dissipation can be found to be

$$w = \frac{gkC_p(1-i)}{\nu \cosh^2 kh}. \tag{4.7}$$

Of the dissipation mechanisms, that due to breaking is always activated in the model when the wave height reaches the breaking criterion. The other dissipation mechanisms can be activated by the user. Dissipation due to waves interacting with a viscous mud bottom is not included.

4.1.2. Lateral Boundary Conditions

Because the model is parabolic, it requires an initial condition and the specification of lateral boundary conditions. These lateral boundary conditions can be of two types in REF/DIF1; open or closed.

Closed lateral boundaries would be relevant for cases where the wave were propagating into a harbor or were bounded by seawalls or headlands. The closed lateral boundary is specified simply as

$$\frac{\partial A}{\partial y} = 0. \tag{4.8}$$

Open lateral boundaries are somewhat more problematic. As of yet there exists no lateral boundary condition implementation for parabolic models that will allow scattered waves over a variable depth to completely leave the domain. Dalrymple and Martin (1992) have developed the "perfect" boundary condition for constant depth wave propagation as simulated by parabolic models and maintain that extension to variable water depth can be performed by using a coordinate transformation in the manner of Liu and Mei (1976); however, this has not been incorporated into numerical models yet, and it is not clear that the coordinate transformation allows straightforward numerical solution. Kirby (1986c) developed a transmitting boundary condition that assumes that Snell's Law (Eq. (3.5) but in a different form) is valid at the boundary

$$\frac{\partial A}{\partial y} = ikA \sin\theta, \tag{4.9}$$

where the right side is derived from Snell's Law. This boundary condition is only perfectly transmitting for plane waves. This open boundary condition is implemented in REF/DIF1.

4.1.3. Resolution Tuning

The model REF/DIF1 has the ability to automatically increase grid resolution in the x direction where appropriate. The model seeks to maintain at least 5 points per wavelength in the x direction. This

resolution is important to model performance since the parabolic approximation assumes that waves are propagating primarily in the x direction.

This increase in resolution can either be performed by the users (for areas where high resolution is required) or by the model. User-specified resolution increases can be done by either specifying a subgrid of increased resolution within the domain or by specifying the number of additional grid rows between reference grid rows (i.e., between grid rows where the bathymetry and currents are specified). If left to the model, a maximum resolution of 5 points per wavelength is possible. Linear interpolation is used between reference gridpoints to calculate values of depth and current at the additional gridpoints created by the resolution increase.

In the y direction, there are no provisions for model-specified resolution adjustments. Increases in resolution in this direction are left to the user in the form of specifying the number of subdivisions between reference values in this direction.

4.1.4. Offshore Islands

Kirby and Dalrymple (1986a) considered the modeling of wave transformation and dissipation around offshore islands and other surface-piercing features using parabolic models. Clearly, the parabolic models cannot account for the backward-propagating reflected wave generated by the island; however, it was felt that the parabolic model should be able to reasonably simulate the wave transformation effects in the lee of the island.

For offshore islands or structures with a sufficiently mild slope to allow waves to break, Kirby and Dalrymple (1986a) introduced the "thin-film" approximation. In it, the water depth over the island was assumed to be sufficiently small that waves breaking at the seaward edge of the island would essentially have zero energy at the leeward edge. This would be equivalent to the island blocking the part of the wave that intersects it. In REF/DIF1, the thin film is 1 cm.

4.1.5 Weak Nonlinearity

As noted in a previous section, the model REF/DIF1 has weak cubic nonlinearity (cubic because of the triple product of unknown amplitudes $|A|^2A$). This weak nonlinearity is a result from Stokes third-order wave theory and was first derived for use in a parabolic mild slope model by Kirby and Dalrymple (1983a). There is no provision for wave-wave interaction between frequencies in the model; this nonlinearity is a self interaction. This nonlinearity primarily affects the wave propagation speed, since nonlinear waves move faster and refract less than their linear counterparts. Strictly, this nonlinearity is valid only in deep water. However, in the interest of creating a useful predictive tool, Kirby and Dalrymple (1986b) developed an asymptotic dispersion relation that matched the nonlinear Stokes solution in deep water and solitary wave theory in shallow. Based on the work of Hedges (1976), the approximate dispersion relation reads

$$\omega^2 = gk\,(1 + D\tanh^5 kh)\tanh\left(kh + \left(\frac{kh}{\sinh\ kh}\right)^4\right), \tag{4.10}$$

where D is given in Eq. (2.24). The formulation of Hedges (1976) is simply a match between linear theory and solitary wave theory. The match between Stokes theory and solitary wave theory in intermediate water depth is not perfect and is not expected to be since the assumptions used to

derive either theory are contradictory to the other. However, Kirby and Dalrymple (1986b) show that the dispersion relation (Eq. 4.10) matches both theories well in their respective areas of validity.

4.1.6 Input Conditions

REF/DIF1 accepts input data at the offshore boundary. This can be done in two ways. The most common method is to specify the incident wave height (actually wave amplitude a, defined as half the incident wave height), angle, and period directly; the model will then convert it to complex amplitudes along the offshore boundary via the following relation

$$A(0, y) = ae^{ik \sin \theta y} . \tag{4.11}$$

Note that there is no integral in the exponential argument; this assumes that the water depths are constant along the y direction at the offshore boundary so that the wave is still a plane wave at input.

Another method of incorporating wave input into REF/DIF1 is by calculating the offshore complex amplitudes external to the model. If the amplitudes and/or water depths vary along the initial boundary, the initial condition can be calculated by

$$A(0, y) = a(y)e^{i\psi(y)} , \tag{4.12}$$

where

$$\psi(y) = \int_0^y k(y) \sin \theta(y)\, dy . \tag{4.13}$$

This would be used if, for example, the initial amplitudes represented a deep-water plane wave that has refracted to the offshore boundary, along which the water depths are different.

4.2 Features in RCPWAVE

4.2.1 Energy Dissipation

RCPWAVE has the same breaking mechanism as REF/DIF1: the wave decay model of Dally et al. (1985). The incipient breaking criterion is different, however; while REF/DIF1 assumes that waves break when the wave height to water depth ratio is 0.78, RCPWAVE uses the somewhat more complex expression of Weggel (1972)

$$\frac{H}{h} = \frac{b}{1 + \dfrac{ba}{gT^2}} , \tag{4.14}$$

where

$$a = 43.75(1 - e^{-19m}) \tag{4.15}$$

$$b = \frac{1.56}{1 + e^{-19.5m}} \tag{4.16}$$

and m is the bottom slope. This expression was developed from analysis of several laboratory studies of incipient breaking. For the case of a flat bottom, the expression reduces to the 0.78 ratio. Additionally, the dissipation in the model takes the angle of propagation into account; thus, the model can refract the waves in the surf zone. This is not done in REF/DIF1; the dissipation occurs in the x direction only. RCPWAVE does not account for dissipation caused by bottom friction or surface films, wave-current interaction, or any nonlinearity.

4.2.2. Lateral Boundary Conditions

RCPWAVE retains only open lateral boundary conditions. It is assumed that the wave heights and the wave angles at the lateral boundaries are equal to those one gridpoint inside the domain. The formulation makes this sufficient for the open lateral condition since the amplitudes are real; for the complex amplitude REF/DIF1 the phase of the complex amplitude must be accounted for in the specification. The lateral boundary conditions in RCPWAVE have the same limitations as those in REF/DIF1.

4.2.3. Resolution Tuning

RCPWAVE does not have the same self-correction of resolution as that of REF/DIF1. It can, however, run on a stretched coordinate grid that is formulated externally to the model. The primary requirement for resolution in RCPWAVE is that the grid be fine enough such that energy always propagates through the front face of the grid cell rather than through the side. Figure 7 illustrates this.

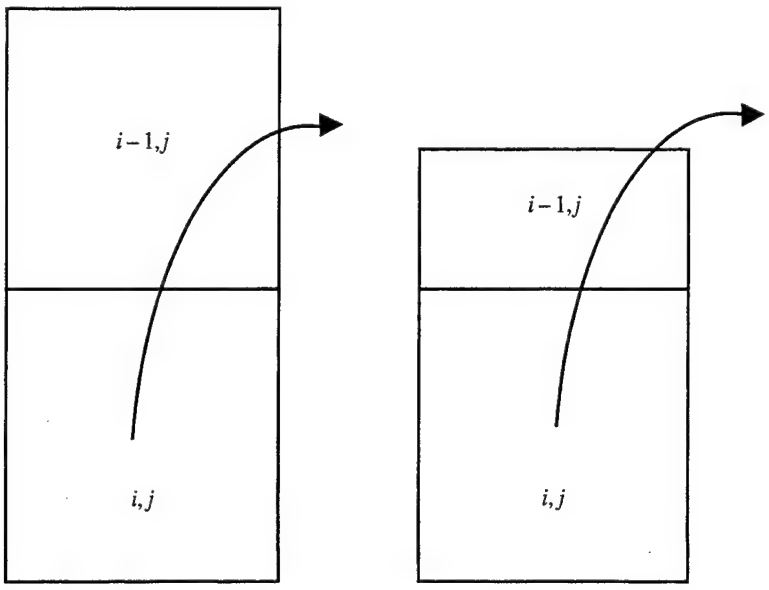

Fig. 7 — Example of resolution requirement in RCPWAVE. Arrows represent paths of energy propagation. (a) Energy propagates through cell side at $i - 1,j$; cell block too large and (b) energy propagates through front face of cell.

4.2.4. Input Conditions

RCPWAVE accepts deep-water conditions for input, not conditions at the offshore boundary. Snell's Law is then used internally to refract the wave conditions from deep water to the edge of the grid. Thus, the model can accept either a plane wave at the offshore boundary or a deep-water plane wave that has refracted to the offshore boundary (along which the depths vary); unlike REF/DIF1, the particular case is transparent to the user.

4.3 Features in REF/DIF-S

4.3.1. Dissipation

The model REF/DIF-S, as stated in a prior section, is a model that can simultaneously propagate waves with different heights, periods and directions over a domain. It is a spectral model in a sense, but different from the traditional definition of a spectral (i.e., phase-averaged) model. In models such as WAM or SWAN, the wave field is assumed to be a statistical quantity at the outset. In REF/DIF-S, the wave field is assumed to be deterministic and statistical measures of wave height are determined from the results. Thus, the wave breaking and dissipation mechanisms need to account for the irregularity of the wave field.

The model used for the spectral dissipation is the "simple model" of Thornton and Guza (1983). The dissipation in the model can be written generically as

$$\frac{\partial A_n}{\partial x} = -\alpha_n A_n , \tag{4.17}$$

where α is the dissipation and n is the index for the wave component. The expression for α is

$$\alpha_n = F\tilde{\beta}_n , \tag{4.18}$$

where

$$\tilde{\beta}_n = \frac{3\sqrt{\pi}}{4\sqrt{g\bar{h}}} \frac{\beta^3 \bar{f} H_{rms}^5}{\gamma^4 h^5} \tag{4.19}$$

and the free parameters B, $\bar{f}$, F, and γ are set as 1.0, f_{peak}, 1.0, and 0.6, respectively (in actuality, $\bar{f}$ is not a free parameter, since Thornton and Guza (1983) defined it as the average frequency; however, for a broad-banded spectrum, it is not clear immediately what the average frequency is so we use the spectral peak). The dissipation does not rely on the initiation of breaking; thus, the dissipation is always turned on, with small values of dissipation calculated where it is essentially zero. This dissipation function was first introduced to a wave shoaling model by Mase and Kirby (1992).

Recently there has been some debate over the structure of the dissipation model, particularly with respect to the distribution of dissipation over the frequency range. The expression (4.18) assumes that the dissipation α_n is not a function of frequency, a view shared by Eldeberky and Battjes (1996) with respect to their own breaking model. More recent work by Kaihatu and Kirby

(1995) and Kirby and Kaihatu (1996) demonstrate that, in fact, the distribution should be a function of frequency squared. This would change Eq. (4.18) to

$$\alpha_n = \alpha_{n0} + \left(\frac{f_n}{f_{peak}}\right)^2 \alpha_{n1}\,, \tag{4.20}$$

where

$$\alpha_{n1} = (\tilde{\beta} - \alpha_{n0}) \frac{f_{peak}^2 \sum_{n=1}^{N} |A_n|^2}{\sum_{n=1}^{N} f_n^2 |A|^2} \tag{4.21}$$

and α_{n0} is given by Eq. (4.19). Kaihatu and Kirby (1995) used $F = 0.5$ for their simulations; this places half the dissipation in a nonfrequency-dependent mechanism and the remaining half in a mechanism that is weighted proportional to f^2. Kirby and Kaihatu (1996) revisited the problem and reasoned that the dissipation not only needs to be weighted more at the higher frequencies, but also that the dependence should be proportional to frequency squared. They used the following reasons to explain these findings:

- Resonant triad interactions in the nearshore area tends to more readily move energy from low frequencies to high. However, experiments of irregular shoaling and breaking waves (e.g., Mase and Kirby 1992) have determined that the spectrum in the surf zone does not become appreciably white. Thus, the dissipation must be weighted heavier on higher frequencies to balance the energy buildup from lower frequencies and nonlinear interactions.
- Time series profiles of surf zone waves resemble triangles. The Fourier transform of these triangles yields coefficients whose sizes are proportional to f^{-1}. The energy density spectrum for the surf zone waves then resemble f^{-2}. To balance this dependence in the higher frequencies, the dissipation needs to be proportional to f^2.

For REF/DIF-S, the form (4.18) with $F = 1.0$ will be retained; this is because the model is at present linear (or, more accurately, has no wave-wave interaction mechanism). The lack of the nonlinear energy transfer would preclude simulation of the processes required for the emphasized weighting of the higher frequency dissipation. A version of REF/DIF-S with triad wave-wave interactions is presently being developed; this model will then require the alternate frequency distribution (4.20) of the dissipation for the reasons stated above. With the exception of breaking and dissipation, REF/DIF-S shares the same features as REF/DIF1.

5.0 CONCLUSIONS

In this report, some of the relevant theory behind numerical modeling of waves in the nearshore area have been outlined. This included a discussion of the mild slope equation, the relevant approximations to this equation (parabolic approximation, eikonal-transport equations), and some of the numerical considerations involved in modeling the equations. Turning the discussion specifically to the models REF/DIF1, REF/DIF-S, and RCPWAVE, some of the relevant physical mechanisms required in these models to accurately simulate wave propagation in shallow water, and the respective

representation and implementation of these effects have been described. In Part 2 of this report, some verification exercises undertaken to validate model performance will be described.

6.0 ACKNOWLEDGMENTS

This report is a result of research conducted under the Naval Research Laboratory (NRL) Core 6.2 "Coastal Simulation" project, funded by the Office of Naval Research, Program Element 0602435N. Discussions with Dr. Y. Larry Hsu (Oceanography Division, NRL) and Mr. W. Erick Rogers (Planning Systems Inc.) have augmented this work.

7.0 REFERENCES

Berkhoff, J. C. W., "Computation of Combined Refraction-Diffraction," *Proceedings of the 13th International Conference on Coastal Engineering*, Vancouver, BC, 471–490, 1972.

Booij, N., *Gravity Waves on Water with Non-Uniform Depth and Current*, Ph.D. dissertation, Technical University of Delft, the Netherlands, 131 p., 1981.

Booij, N. "A Note on the Accuracy of the Mild-Slope Equation," *Coastal Engineering* **7**, 191–203 (1983).

Carnahan, B., H. A. Luther, and J. O. Wilkes, *Applied Numerical Methods*, John Wiley and Sons, New York, NY, 604 p., 1969.

Chawla, A., *Wave Transformation over a Submerged Shoal*, M.S. thesis, Center for Applied Coastal Research, University of Delaware, Newark, DE, 240 p., 1995.

Chen, H. S. and J. R. Houston, "Calculation of Water Oscillation in Coastal Harbors: HARBS and HARBD User's Manual," Instruction report CERC-87-2, Coastal Engineering Research Center, U.S. Army Corps of Engineers Waterways Experiment Station, 31 p., 1987.

Dally, W. R., R. G. Dean, and R. A. Dalrymple, "Wave Height Variations Across Beaches of Arbitrary Profile," *Journal of Geophysical Research* **90**, 11,917–11,927 (1985).

Dalrymple, R. A., J. T. Kirby, and P. A. Hwang, "Wave Diffraction Due to Areas of Energy Dissipation," *Journal of Waterways, Ports, Coastal, and Ocean Engineering* **110**, ASCE, 67–79 (1984).

Dalrymple, R. A. and P. A. Martin, "Perfect Boundary Conditions for Parabolic Water-Wave Models," *Proceedings of the Royal Society of London*, Series A, **437**, 41–54 (1992).

Dean, R. G. and R. A. Dalrymple, *Water Wave Mechanics for Engineers and Scientists*, Prentice-Hall, Englewood Cliffs, NJ, 353 p., 1984.

Ebersole, B. A., "Refraction-Diffraction Model for Linear Water Waves," *Journal of Waterways, Ports, Coastal, and Ocean Engineering* **111**, ASCE, 939–953 (1985).

Ebersole, B. A., M. A. Cialone, and M. D. Prater, "Regional Coastal Processes Numerical Modeling System Report 1: RCPWAVE – A Linear Wave Propagation Model for Engineering Use," Technical Report CERC-86-4, Coastal Engineering Research Center, U.S. Army Corps of Engineers Waterways Experiment Station, Vicksburg, MS, 71 p., 1986.

Eldeberky, Y. and J. A. Battjes, "Spectral Modeling of Wave Breaking: Application to Boussinesq Equations," *Journal of Geophysical Research* **101**, 1253–1264 (1996).

Hedges, T. S., "An Empirical Modification to Linear Wave Theory," *Proceedings of the Institute of Civil Engineering* **61**, 575–579 (1976).

Holthuijsen, L. H., N. Booij, and R. C. Ris, "A Spectral Wave Model for the Coastal Zone," *Proceedings of the 2nd International Symposium on Ocean Wave Measurement and Analysis*, New Orleans, LA, 630–641 (1993).

Kaihatu, J. M. and J. T. Kirby, "Nonlinear Transformation of Waves in Finite Water Depth," *Physics of Fluids* **7**, 1903–1914 (1995).

Kirby, J. T., "A Note on Linear Surface Wave-Current Interaction," *Journal of Geophysical Research* **89**, 745–747 (1984).

Kirby, J. T., "Higher-Order Approximations in the Parabolic Equation Method for Water Waves," *Journal of Geophysical Research* **91**, 933–952 (1986a).

Kirby, J. T., "Rational Approximations in the Parabolic Equation Method for Water Waves," *Coastal Engineering* **10**, 355–378 (1986b).

Kirby, J. T., "Open Boundary Condition in Parabolic Equation Method," *Journal of Waterways, Ports, Coastal, and Ocean Engineering* **112**, 460–465 (1986c).

Kirby, J. T., "Discussion of 'Refraction-Diffraction Model for Linear Water Waves,' by B. A. Ebersole," *Journal of Waterways, Ports, Coastal, and Ocean Engineering* **114**, ASCE, 101–103 (1988).

Kirby, J. T. and R. A. Dalrymple, "A Parabolic Equation for the Combined Refraction-Diffraction of Stokes Waves by Mildly Varying Topography," *Journal of Fluid Mechanics* **136**, 543–566 (1983a).

Kirby, J. T. and R. A. Dalrymple, "Propagation of Weakly Nonlinear Surface Waves in the Presence of Varying Depth and Currents," *Proceedings of the 20th Congress, International Association on Hydraulic Research*, Moscow, Russia, 198–202, 1983b.

Kirby, J. T. and R. A. Dalrymple, "Modeling Waves in Surfzones and Around Islands," *Journal of Waterways, Ports, Coastal, and Ocean Engineering* **112**, ASCE, 78–93 (1986a).

Kirby, J. T. and R. A. Dalrymple, "An Approximate Model for Nonlinear Dispersion in Monochromatic Wave Propagation Models," *Coastal Engineering* **9**, 545–561 (1986b).

Kirby, J. T. and R. A. Dalrymple, "Combined Refraction/Diffraction Model REF/DIF1, Version 2.5: Documentation and User's Manual," CACR Report 94-22, Center for Applied Coastal Research, University of Delaware, Newark, DE, 171 p., 1994.

Kirby, J. T. and J. M. Kaihatu, "Structure of Frequency Domain Models for Random Wave Breaking," *Proceedings of the 25th International Conference on Coastal Engineering*, Orlando, FL, 1144–1155, 1996.

Kirby, J. T. and H. T. Ozkan, "Combined Refraction/Diffraction Model for Spectral Wave Conditions REF/DIF-S, Version 1.1: Documentation and User's Manual," CACR Report 94-04, Center for Applied Coastal Engineering, University of Delaware, Newark, DE, 128 p., 1994.

Komen, G. J., L. Cavaleri, M. Donelan, K. Hasselmann, S. Hasselmann, and P. A. E. M. Janssen, *Dynamics and Modeling of Ocean Waves*, Cambridge University Press, Cambridge, UK, 532 p., 1994.

Liu, P. L.-F., "Parabolic Wave Equation for Surface Water Waves," Miscellaneous report CERC-86-11, Coastal Engineering Research Center, U.S. Army Corps of Engineers Waterways Experiment Station, Vicksburg, MS, 32 p., 1986.

Liu, P. L.-F. and C. C. Mei, "Water Motions on a Beach in the Presence of a Breakwater. 1. Waves," *Journal of Geophysical Research* **81**, 3079–3084 (1976).

Lozano, C. J. and P. L.-F. Liu, "Refraction-Diffraction Model for Linear Surface Water Waves," *Journal of Fluid Mechanics* **101**, 705–720 (1980).

Mase, H. and J. T. Kirby, "Hybrid Frequency-Domain KdV Equation for Random Wave Transformations," *Proceedings of the 23rd International Conference on Coastal Engineering*, Venice, Italy, 474–487, 1992.

Munk, W. H. and R. S. Arthur, "Wave Intensity Along a Refracted Ray in Gravity Waves," Circular 521, National Bureau of Standards, 95–108, 1952.

Phillips, O. M., *The Dynamics of the Upper Ocean* (2nd Edition), Cambridge University Press, Cambridge, UK, 336 p., 1980.

Radder, A. C., "On the Parabolic Equation Method for Water Wave Propagation," *Journal of Fluid Mechanics* **95**, 159–176 (1979).

Reid, R. O. and K. Kajuira, "On the Damping of Gravity Waves Over a Permeable Seabed," *Transactions of the American Geophysical Union* **38**, 662 (1957).

Resio, D. T., "A Steady State Model for Coastal Applications," *Proceedings of the 21st International Conference on Coastal Engineering*, Malaga, Spain, 929–940, 1988.

Smith, R. and T. Sprinks, "Scattering of Surface Waves by a Conical Island," *Journal of Fluid Mechanics* **72**, 373–384 (1975).

Thornton, E. B. and R. T. Guza, "Transformation of Wave Height Distribution," *Journal of Geophysical Research* **88**, 5925–5938 (1983).

Weggel, J. R., "Maximum Breaker Height," *Journal of the Waterways, Harbors, and Coastal Engineering Division* **78**, ASCE, 529–548 (1972).

Xu, B., V. Panchang, and Z. Demirbilek, "Exterior Reflections in Elliptic Harbor Wave Models," *Journal of Waterways, Ports, Coastal, and Ocean Engineering* **122**, ASCE, 118–126 (1996).

Yue, D. K. P. and C. C. Mei, "Forward Diffraction of Stokes Waves by a Thin Wedge," *Journal of Fluid Mechanics* **99**, 33–52 (1980).